Visibly Transparent Polymer Solar Cells Produced by Solution Processing

Chun-Chao Chen,[†,⊥] Letian Dou,[†,⊥] Rui Zhu,[†,*] Choong-Heui Chung,[†] Tze-Bin Song,[†] Yue Bing Zheng,[‡,§] Steve Hawks,[†] Gang Li,[†] Paul S. Weiss,[‡,§,*] and Yang Yang[†,‡,*]

[†]Departments of Materials Science and Engineering, [‡]California NanoSystems Institute, and [§]Departments of Chemistry and Biochemistry, University of California, Los Angeles, Los Angeles, California 90095, United States. [⊥]These authors contributed equally to the work.

ABSTRACT

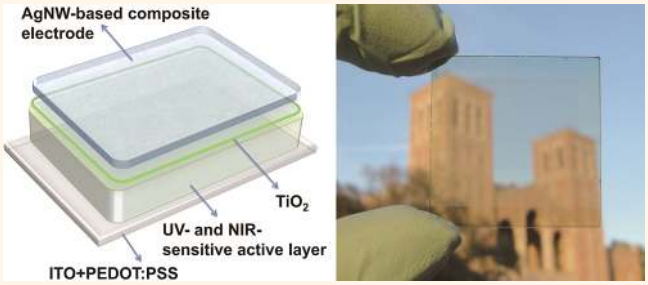

Visibly transparent photovoltaic devices can open photovoltaic applications in many areas, such as building-integrated photovoltaics or integrated photovoltaic chargers for portable electronics. We demonstrate high-performance, visibly transparent polymer solar cells fabricated *via* solution processing. The photoactive layer of these visibly transparent polymer solar cells harvests solar energy from the near-infrared region while being less sensitive to visible photons. The top transparent electrode employs a highly transparent silver nanowire–metal oxide composite conducting film, which is coated through mild solution processes. With this combination, we have achieved 4% power-conversion efficiency for solution-processed and visibly transparent polymer solar cells. The optimized devices have a maximum transparency of 66% at 550 nm.

KEYWORDS: transparent solar cell · transparent electrode · silver nanowire · solution process · polymer solar cell

Polymer solar cells (PSCs) have drawn intense attention due to their advantages over competing solar cell technologies.[1−3] Current progress in the power-conversion efficiency (PCE) of PSCs has reached a new record of 10.6% based on tandem architecture,[3] demonstrating the promising future of PSCs as low-cost and efficient photovoltaic (PV) candidates for solar energy harvesting. In addition to the pursuit of high device efficiency, PSCs have also been intensely investigated for their potential in making unique advances for broader applications.[3−5] Several such applications would be enabled by high-performance *visibly transparent* PV devices, including building-integrated photovoltaics (BIPV)[6] and integrated PV chargers for portable electronics.[7] Previously, many attempts have been made toward demonstrating visibly transparent or semitransparent PSCs.[8−17] Transparent conductors, such as thin metal films, metallic grids, metal nanowire networks, metal oxides, conducting polymers, and graphene, have been deposited onto photoactive layers as top electrodes to achieve visibly transparent or semitransparent PSCs. However, these demonstrations often result in low visible light transparency and/or low device efficiency, because suitable polymeric PV materials and efficient transparent conductors were not well deployed in device design and fabrication.

From the PV materials point of view, an ideal photoactive layer material for visibly transparent PSCs needs to harvest most of the photons from ultraviolet (UV) and near-infrared (NIR) wavelengths in the solar spectrum, while the photons in the visible range should be transmitted. Since high power conversion efficiency is strongly dependent on the fraction of photons absorbed, there is often a compromise between captured photons and polymeric film transparency that limits materials development for visibly transparent PSCs. For example, poly(3-hexylthiophene) (P3HT):[6,6]-phenyl-C61–butyric acid methyl ester (PCBM) blend is the most commonly used photoactive layer material in visibly semitransparent PSCs.[11] However, due to its efficient photon harvesting in the visible wavelength region, P3HT:PCBM (and many other) devices often have low visible transparency. On the other hand, the transparent conductor is another key factor that determines the performance of visibly transparent PSCs. An ideal transparent conductor for visibly transparent PSCs must simultaneously have high transparency and low resistance together with ease of processing and effective charge collecting. However, a trade-off is often

* Address correspondence to iamzhurui@gmail.com (R.Z.), psw@cnsi.ucla.edu (P.S.W.), yangy@ucla.edu (Y.Y.).

Received for review May 21, 2012 and accepted July 3, 2012.

Published online 10.1021/nn3029327

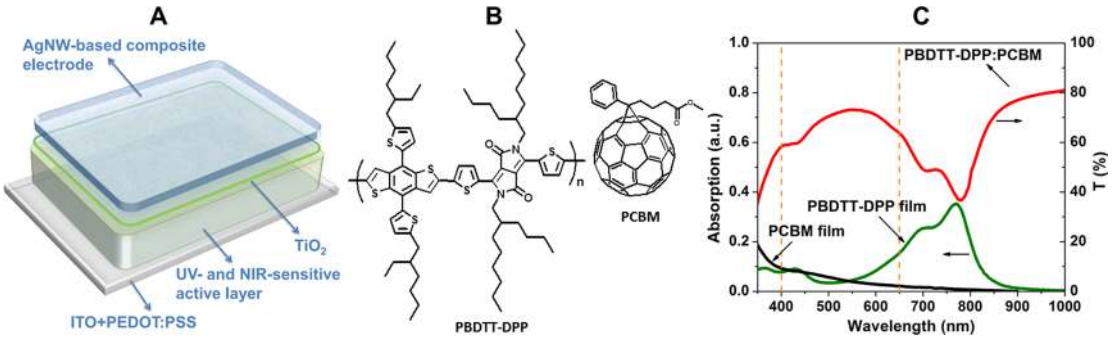

Figure 1. (A) Schematic of the device architecture for solution-processed visibly transparent polymer solar cells. (B) Chemical structure of the donor (PBDTT-DPP) and acceptor (PCBM) materials used for the UV- and NIR-sensitive active layer. (C) Absorption spectra of PBDTT-DPP and PCBM and transmission spectrum of the PBDTT-DPP:PCBM bulk heterojunction photoactive layer. The dashed lines indicate the visible wavelength region.

found with these electrode materials, as high conductivity often sacrifices transparency.[18] For example, thermally evaporated thin metallic films are commonly used as semitransparent electrodes for PSCs, but the conductivity is significantly compromised by the film transparency.[9] Some recently developed solution-processable conductive materials, such as carbon nanotubes,[19,20] graphene,[21,22] poly(3,4-ethylenedioxythiophene):poly(styrene sulfonate) (PEDOT:PSS),[23−25] and silver nanowires (AgNWs),[26−29] have opened up a new era for transparent conductors. Despite the unique advantages of these candidates, they all have drawbacks limiting their applications in visibly transparent PSCs. For example, one major drawback is the damage caused by these transparent conductors to the underlying, soft polymeric photoactive layers during their deposition. Other issues include the chemical, physical, mechanical, or energetic incompatibility between the polymeric photoactive layer and the transparent conductor that can lead to the low performance or low transparency of the visibly transparent PSCs reported to date.

In this work, we demonstrate a solution to overcome the aforementioned challenges for visibly transparent PSCs. High-performance visibly transparent PSCs are achieved by combining polymeric PV materials sensitive to NIR light but highly transparent to visible light, together with solution-processed high-performance AgNW-based composite transparent conductors. Both visible light transparency and PCE are addressed simultaneously. Finally, a solution-processed and highly transparent solar cell is demonstrated with a PCE of 4% and a maximum transmission of ~66% at 550 nm.

RESULTS AND DISCUSSION

Figure 1A shows the schematic structure of a visibly transparent PSC. An UV and NIR light-sensitive photoactive layer is sandwiched between two transparent electrodes. The photoactive layer is a bulk heterojunction blend consisting of the NIR light-sensitive PV polymer poly(2,6′-4,8-bis(5-ethylhexylthienyl)benzo-[1,2-*b*;3,4-*b*]dithiophene-*alt*-5-dibutyloctyl-3,6-bis(5-bromothiophen-2-yl)pyrrolo[3,4-*c*]pyrrole-1,4-dione) (PBDTT-DPP, Figure 1B)[30] as the electron donor and PCBM as electron acceptor. Figure 1C shows the film absorption of PBDTT-DPP, PCBM, and their blend. PBDTT-DPP is a low band gap polymer with strong photosensitivity in the range 650−850 nm, while the absorption of PCBM is located below 400 nm. With these two materials in combination, the PBDTT-DPP:PCBM photoactive layer has a maximum transmission of 73% at ~550 nm and an average transmission of 68% over the entire visible range (400 to 650 nm), but is strongly absorbing in the NIR range (from 650 to 850 nm), as shown in Figure 1C. This spectral coverage of PBDTT-DPP:PCBM film ensures harvesting of UV and NIR photons while most visible photons are transmitted, making for an excellent candidate for the visibly transparent PSCs.

For transparent conductors, both the bottom and top electrodes require high transparency to ensure the transmission of visible light. We define the electrode deposited onto the photoactive layer as the top electrode and the electrode on which the photoactive layer is coated as the bottom electrode. Commercial indium−tin-oxide (ITO) substrates can be chosen as the bottom anode electrode, which is often covered by PEDOT:PSS as an anode-modification layer. However, great challenges remain for the high-performance transparent top cathode that is to be deposited on top of the photoactive layer. The dominant reason is the aforementioned compatibility issue, because polymer or organic films are often too thin and soft to survive the deposition processes required for most transparent conductors. To solve this problem, a spray-coated AgNW-based composite is applied in our approach to achieve the high-performance top transparent cathode. The AgNWs can be spray-coated onto the photoactive layer through alcohol-based solvents, which are compatible with common PSC materials. The AgNW network is then fused using a TiO_2 sol−gel solution to enhance the connection between AgNWs and the adhesion of AgNWs to the underlying photoactive layers.[29] This step is performed with mild

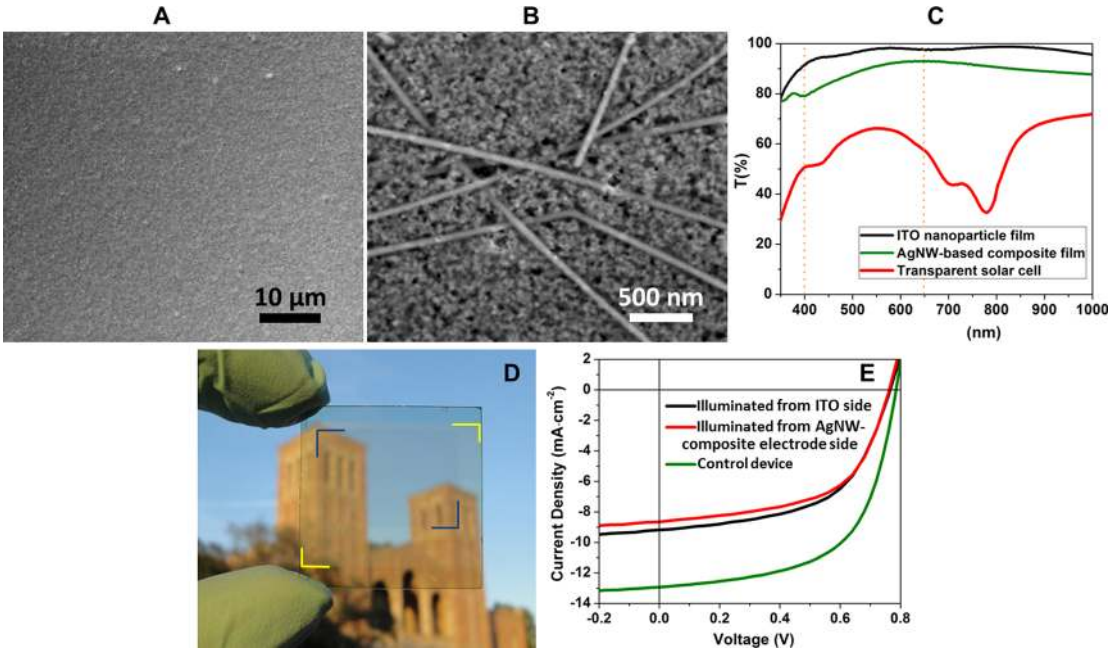

Figure 2. SEM images of the top (A) and bottom (B) surfaces of the AgNW-based composite transparent electrode. (C) Transmission spectra of the pristine ITO nanoparticle film, the AgNW-based composite transparent electrode, and a visibly transparent polymer solar cell. (D) Photograph of a visibly transparent polymer solar cell. The yellow and blue brackets indicate the top AgNW-based composite electrode and the bottom ITO electrode, respectively. (E) Current density−voltage characterization of the transparent device (illuminated from ITO side or AgNW composite electrode side) and the control device (using reflective thermal-evaporated Al as top electrode).

processing conditions and has good compatibility with the photoactive layer. Transparent conductive fillers are placed in the empty space in the crossed AgNW conducting network.[31] The conductive filler is designed to extract the charges generated from areas that are not covered by AgNWs and transport these charges to the AgNW matrix. We chose ITO nanoparticles as the filler for the AgNW network to form the AgNW-based composite transparent conductor. The ITO-based filling material also contains a polymeric binder that can improve the adhesion of AgNW networks onto the photoactive layer and form a continuous film with good contact with the underlying active layer. Figure 2A shows the scanning electron microscopic (SEM) image of the top surface of the AgNW-based composite electrode. The AgNW networks are completely buried in the ITO nanoparticle-based conductive filling material, resulting in a smooth top surface. By using a "floating-off" technique,[32] the composite transparent electrode can be flipped to expose the bottom surface, which is in contact with the underlying photoactive layer. Figure 2B shows a SEM image of the bottom surface of the composite transparent conductor. The AgNWs from the bottom surface are exposed to the active layer, which indicates that ITO nanoparticles did not diffuse into the contact area between AgNWs and the active layer, but only filled the hollow space between the AgNWs. Figure 2C shows the transmittance spectra of the ITO nanoparticle film alone and the AgNW-based composite film containing ITO nanoparticle fillers. The ITO nanoparticle film (thickness ~400 nm) alone has high transparency within the visible and NIR range and low sheet resistance of ~100 kΩ/□ measured *via* four-point probe measurements. The pristine AgNWs films prepared by spray-coating methods have resistances of >1 MΩ/□ initially. After being treated with the TiO_2 sol−gel solution and further coated by the ITO nanoparticle fillers, the resulting AgNW composite films have an average transmittance of ~87% from 400 to 1000 nm with sheet resistances of ~30 Ω/□. These results have met the requirements for the top cathode of a visibly transparent PSC.

Between the active layer and top electrode, a suitable interface modification layer is also critical. The interlayer not only acts as a protective film on the soft photoactive layer but also reduces the energy barrier for carrier transport from photoactive layer to top electrode. Here, we deposited a 20-nm-thick TiO_2 nanoparticle from a sol−gel solution on top of the photoactive layer to act as cathode interfacial layer.[33,34] The TiO_2 nanoparticle layer prevents the silver nanowire from damaging the underlying soft films. Moreover, owing to its photoconductivity and proper work function alignment with the photoactive polymer material, the TiO_2 nanoparticle layer serves as an efficient electron-transporting layer and allows electrons to tunnel through the energy barrier into the AgNW-based electrode.

Based on the above structure, we produced solution-processed and visibly transparent PSCs with an average light transmission of 61% over the 400 to

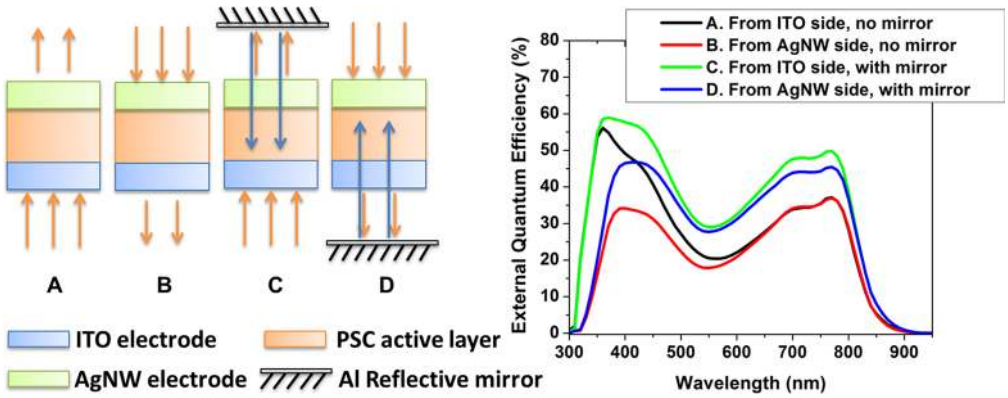

Figure 3. External quantum efficiency (EQE) characterization of the visibly transparent PSC with different testing methods. The incident light beam illuminated from both ITO (A) and AgNW (B) electrode sides were investigated. An Al-based reflective mirror was then placed at the back of the transparent device to reflect the transmitted photons back to the device (C and D), and the EQE spectra were also collected. The calculated J_{sc} values based on the EQE results for these tests are (A) 8.99 mA·cm^{-2}; (B) 8.24 mA·cm^{-2}; (C) 12.16 mA·cm^{-2}; and (D) 11.01 mA·cm^{-2}.

650 nm range and a maximum transmission of 66% at ~550 nm (Figure 2C). Figure 2D shows a photograph of a highly transparent PSC where the buildings behind can be clearly seen through the device. The yellow and blue brackets indicate the edge of the top AgNW-based composite electrode and the bottom ITO electrode, respectively. Figure 2E demonstrates the current density−voltage (J−V) curves of this visibly transparent PSC measured under simulated AM 1.5G illumination with an intensity of 1000 W·m^{-2}. The performance of a control device is also shown in Figure 2E, which uses evaporated Al as a reflective top electrode. For the control device, a power conversion efficiency of 6.03% was obtained with a short-circuit current density (J_{sc}) of 13.0 mA·cm^{-2}, an open-circuit voltage (V_{oc}) of 0.78 V, and a fill factor (FF) of 59.5%. In the testing of the visibly transparent PSCs, we measured the device performance with illumination from either the ITO substrate side or the top AgNW-composite transparent conductor side. When illuminated from the ITO substrate side, a PCE of 4.02% was achieved with V_{oc} = 0.77 V, J_{sc} = 9.3 mA·cm^{-2}, and FF = 56.2%. When the device test was performed with illumination from the top AgNW-composite electrode side, similar performance was obtained: V_{oc} = 0.76 V, J_{sc} = 8.7 mA·cm^{-2}, FF = 57.8%, and PCE = 3.82%. Both measurements show similar V_{oc} and FF. The only difference comes from the J_{sc}, which is due to the slightly lower transparency of the AgNW-based composite electrode films as compared to the commercial ITO substrates. To understand the reproducibility of the results obtained, 40 transparent PSCs were prepared and consistent results of PCE between 3.6% and 4% were obtained with illumination from the ITO substrate side. Figure 3 shows the external quantum efficiency (EQE) characterization of the visibly transparent PSCs. J_{sc} can be calculated by integrating the EQE results with the solar spectrum. The J_{sc} obtained by EQE illumination from the ITO and AgNW side are 8.99 and 8.32 mA·cm^{-2}, respectively.

TABLE 1. Summary of Device Performance under Different Testing Conditions As Described in Figure 3

testing conditions	V_{oc} (V)	J_{sc} (mA/cm^2)	FF (%)	PCE (%)
A. From the ITO side, no mirror	0.77	9.30	56.2	4.02
B. From the AgNW side, no mirror	0.76	8.70	57.8	3.82
C. From the ITO side, with reflective mirror	0.77	12.60	54.4	5.28
D. From the AgNW side, with reflective mirror	0.76	11.63	55.7	4.92

These values are roughly consistent with the results obtained from the J−V characterization. Moreover, a reflective mirror can be placed at the back of the visibly transparent PSC to reflect the transmitted photons back to the device, as illustrated in tests C and D of Figure 3. The J_{sc} measured from EQE of tests C and D are 12.16 and 11.01 mA·cm^{-2}, respectively. Table 1 summarizes the J−V characterization of different measurements described in Figure 3. The J_{sc} of 12.60 mA·cm^{-2} obtained from test C is comparable to that of our control devices (13.0 mA·cm^{-2} with a conventional TiO_2/Al electrode). These results show that the photons transmitted through the visibly transparent PSCs can still be utilized for the energy generation or other optical applications, indicating the broad applications of visibly transparent PSCs.

Conclusions and Prospects. We have demonstrated high-performance, solution-processed, visibly transparent polymer solar cells through the incorporation of near-infrared light-sensitive polymer and using silver nanowire composite films as the top transparent electrode. The near-infrared photoactive polymer PBDTT-DPP absorbs more near-infrared light but is less sensitive to visible light, balancing solar cell performance and transparency in the visible wavelength region. The transparent top electrode is a fully solution-processed silver nanowire-based composite film, which is compatible with common PSC materials. With this combination, we have achieved ~4% power-conversion efficiency for the solution-processed and

visibly transparent solar cells, while the devices have high transparency, 66% at 550 nm. These results open the potential for visibly transparent polymer solar cells as add-on components of multijunction photovoltaic devices, smart windows, and building-integrated photovoltaics and in other applications.

METHODS

Materials. The near-infrared light-sensitive active polymer is poly[2,6′-4,8-bis(5-ethylhexylthienyl)benzo[1,2-*b*;3,4-*b*]dithiophene-*alt*-5-dibutyloctyl-3,6-bis(5-bromothiophen-2-yl)pyrrolo[3,4-c]-pyrrole-1,4-dione] (PBDTT-DPP), which was developed in our lab.[30] [6,6]-Phenyl C_{61}-butyric acid methyl ester was purchased from Nano-C (Westwood, MA, USA). Poly(3,4-ethylenedioxythiophene)/poly(styrenesulfonate) (PEDOT:PSS, CLEVIOS P VP AI 4083) was purchased from H. C. Starck (Newton, MA, USA). TiO_2 nanoparticle solutions were prepared according to a previous report.[34] Silver nanowires were purchased from BlueNano Inc. (Charlotte, NC, USA) or Kechuang Advanced Materials Co., Ltd. (Hangzhou, Zhejiang, China). Indium−tin-oxide nanoparticle dispersions were purchased from Aldrich (Milwaukee, WI, USA) or obtained as gifts from Evonik Degussa Corporation (Piscataway, NJ, USA).

Device Fabrication. The device structures are (a) visibly transparent polymer solar cells, ITO/PEDOT:PSS/PBDTT-DPP:PCBM/TiO_2/AgNW composite electrode, and (b) control device, ITO/PEDOT:PSS/PBDTT-DPP:PCBM/TiO_2/Al. Visibly transparent polymer solar cells (a) were fabricated on patterned ITO-coated glass substrates with a sheet resistance of 15 Ω/□. The PEDOT:PSS layer was spin-cast at 4000 rpm for 60 s and annealed at 120 °C for 15 min in air. The PBDTT-DPP:PCBM blend with a weight ratio of 1:2 in dichlorobenzene solution (0.7 wt %) was spin-cast at 2500 rpm for 80 s on top of the PEDOT:PSS layer to form a ∼100-nm-thick active layer. A TiO_2 sol−gel solution was then spin-coated onto the active layer at 2500 rpm for 30 s and annealed at 100 °C for 1 min to form the *n*-type interface layer. For the deposition of the AgNW-based composite electrode, the silver nanowire dispersion in isopropyl alcohol was spin-coated (2 mg/mL dispersion, 2500 rpm, 10 drops) or spray-coated (0.05 mg/mL dispersion) onto the TiO_2 layer to form AgNW conducting networks.[29] The fusing process of the silver nanowire network was then carried out by applying diluted TiO_2 sol−gel solution in ethanol at 3000 rpm and baking at 100 °C for 10 s. The ITO nanoparticle dispersion (10 wt %) was used as transparent conductive filler and was spin-coated onto the fused AgNW matrix to form the composite electrode. Mild heating at 80 °C for 1 min removed the residual solvent. The thickness of the transparent composite electrode is around 400 nm. The device electrode fingers were formed by cutting the films with a blade and blowing the devices with N_2 to avoid possible short circuits between the top AgNWs and the bottom ITO substrate. The active area is 10 mm^2, which is defined by the overlap between bottom ITO substrate and the top fingers. For control device (b) with an evaporated reflective Al electrode, the devices were completed by thermal evaporation of 100 nm Al as the cathode under vacuum at a base pressure of 2×10^{-6} Torr after the deposition of the photoactive polymer layer.

Optical and Electrical Characterization. The transmission spectra were recorded using a Hitachi ultraviolet−visible U-4100 spectrophotometer (Hitachi High-Technologies Corporation, Tokyo, Japan). Current density−voltage characteristics of photovoltaic cells were measured using a Keithley 2400 source unit (Keithley Instruments, Inc., Cleveland, OH, USA) under a simulated AM1.5G spectrum with an Oriel 91191 solar simulator (Newport Corporation, Irvine, CA, USA). The light intensity was ∼100 mW·cm^{-2}, as calibrated using a Si photodiode. The surface resistance (<100 Ω/□) was measured using the four-point probe method with a surface resistivity meter (Guardian Manufacturing, Cocoa, FL, USA, model: SRM-232−100, range: 0−100 Ω/□). Incident photon-to-current conversion efficiency (IPCE) and external quantum efficiency were measured on a custom-made IPCE system. The scanning electron microscopy images were taken using an FEI Nova NanoSEM 650 (FEI Corporation, Hillsboro, OR, USA).

Conflict of Interest: The authors declare no competing financial interest.

Acknowledgment. This research was financially supported by the Engineering School of UCLA, the Office of Naval Research (N00014-04-1-0434, Program Manager: Dr. P. Armistead), and the Kavli Foundation. The authors are grateful to Mr. Yang Yang (student) and Dr. Jingbi You of UCLA for helpful information. C.C.C. would like to thank the NSF-funded IGERT: Clean Energy for Green Industry Fellowship (Grant DGE-0903720). S.A.H. would like to thank the NSF-funded IGERT: Materials Creation Training Program (MCTP, Grant DGE-0654431). G.L. would like to thank the UCLA Henry Samuli School of Engineering and Applied Science for financial support.

REFERENCES AND NOTES

1. Yu, G.; Gao, J.; Hummelen, J. C.; Wudl, F.; Heeger, A. J. Polymer Photovoltaic Cells: Enhanced Efficiencies *via* a Network of Internal Donor-Acceptor Heterojunctions. *Science* **1995**, *270*, 1789–1791.
2. Brabec, C. J.; Gowrisanker, S.; Halls, J. M.; Laird, D.; Jia, S.; Williams, S. P. Polymer Fullerene Bulk-Heterojunction Solar Cells. *Adv. Mater.* **2010**, *22*, 3839–3856.
3. Li, G.; Zhu, R.; Yang, Y. Polymer Solar Cells. *Nat. Photonics* **2012**, *6*, 153–161.
4. Lipomi, D. J.; Tee, B. C. K.; Vosgueritchian, M.; Bao, Z. N. Stretchable Organic Solar Cells. *Adv. Mater.* **2011**, *23*, 1771–1775.
5. Park, H. J.; Xu, T.; Lee, J. Y.; Ledbetter, A.; Guo, L. J. Photonic Color Filters Integrated with Organic Solar Cells for Energy Harvesting. *ACS Nano* **2011**, *5*, 7055–7060.
6. Henemann, A. BIPV: Built-in Solar Energy. *Renewable Energy Focus* **2008**, *9*, 14–19.
7. Zhu, R.; Kumar, A.; Yang, Y. Polarizing Organic Photovoltaics. *Adv. Mater.* **2011**, *23*, 4193–4198.
8. Bailey-Salzman, R. F.; Rand, B. P.; Forrest, S. R. Semitransparent Organic Photovoltaic Cells. *Appl. Phys. Lett.* **2006**, *88*, 233502.
9. Ng, G. M.; Elizabeth, L. K.; Kietzke, T.; Tan, L. W.; Liew, P. K.; Zhu, F. R. Optical Enhancement in Semitransparent Polymer Photovoltaic cells. *Appl. Phys. Lett.* **2007**, *90*, 103505.
10. Huang, J. S.; Li, G.; Yang, Y. A Semi-Transparent Plastic Solar Cell Fabricated by a Lamination Process. *Adv. Mater.* **2008**, *20*, 415–419.
11. Lee, Y. Y.; Tu, K. H.; Yu, C. C.; Li, S. S.; Hwang, J. Y.; Lin, C. C.; Chen, K. H; Chen, L. C.; Chen, H. L.; Chen, C. W. Top Laminated Graphene Electrode in a Semitransparent Polymer Solar Cell by Simultaneous Thermal Annealing/Releasing Method. *ACS Nano* **2011**, *5*, 6564–6570.
12. Ameri, T.; Dennler, G.; Waldauf, C.; Azimi, H.; Seemann, A; Forberich, K.; Hauch, J.; Scharber, M.; Hinger, K.; Brabec, C. J. Fabrication, Optical Modeling, and Color Characterization of Semitransparent Bulk-Heterojunction Organic Solar Cells in an Inverted Structure. *Adv. Funct. Mater.* **2010**, *20*, 1592–1598.
13. Gaynor, W.; Lee, J. Y.; Peumans, P. Fully Solution-Processed Inverted Polymer Solar Cells with Laminated Nanowire Electrodes. *ACS Nano* **2010**, *4*, 30–34.
14. Colsmann, A.; Puetz, A.; Bauer, A.; Hanisch, J.; Ahlswede, E.; Lemmer, U. Efficient Semi-Transparent Organic Solar Cells with Good Transparency Color Perception and Rendering Properties. *Adv. Energy Mater.* **2011**, *1*, 599–603.
15. Lunt, R. R.; Bulovic, V. Transparent, Near-Infrared Organic Photovoltaic Solar Cells for Window and Energy-Scavenging Applications. *Appl. Phys. Lett.* **2011**, *98*, 113305.

16. Meiss, J.; Holzmueller, F.; Gresser, R.; Leo, K.; Riede, M. Near-Infrared Absorbing Semitransparent Organic Solar Cells. *Appl. Phys. Lett.* **2011**, *99*, 193307.
17. Bauer, A.; Wahl, T.; Hanisch, J.; Ahlswede, E. ZnO:Al Cathode for Highly Efficient, Semitransparent 4% Organic Solar Cells Utilizing TiO_x and Aluminum Interlayers. *Appl. Phys. Lett.* **2012**, *100*, 073307.
18. Hecht, D. S.; Hu, L. B.; Irvin, G. Emerging Transparent Electrodes Based on Thin Films of Carbon Nanotubes, Graphene, and Metallic Nanostructures. *Adv. Mater.* **2011**, *23*, 1482–1513.
19. Pasquier, A. D.; Unalan, H. E.; Kanwal, A.; Miller, S.; Chhowalla, M. Conducting and Transparent Single-wall Carbon Nanotube Electrodes for Polymer-Fullerene Solar Cells. *Appl. Phys. Lett.* **2005**, *87*, 203511.
20. Rowell, M. W.; Topinka, M. A.; McGehee, M. D.; Prall, H. J.; Dennler, G.; Sariciftci, N. S.; Hu, L.; Gruner, G. Organic Solar Cells with Carbon Nanotube Network Electrodes. *Appl. Phys. Lett.* **2006**, *88*, 233506.
21. Becerril, H. A.; Mao, J.; Liu, Z.; Stoltenberg, R. M.; Bao, Z.; Chen, Y. Evaluation of Solution-Processed Reduced Graphene Oxide Films as Transparent Conductors. *ACS Nano* **2008**, *2*, 463–470.
22. Tung, V. C.; Chen, L. M.; Allen, M. J.; Wassei, J. K.; Nelson, K.; Kaner, R. B.; Yang, Y. Low-Temperature Solution Processing of Graphene−Carbon Nanotube Hybrid Materials for High-Performance Transparent Conductors. *Nano Lett.* **2009**, *9*, 1949–1955.
23. Kim, Y. H.; Sachse, C.; Machala, M. L.; May, C.; Müller-Meskamp, L.; Leo, K. Highly Conductive PEDOT:PSS Electrode with Optimized Solvent and Thermal Post-Treatment for ITO-Free Organic Solar Cells. *Adv. Funct. Mater.* **2011**, *21*, 1076–1081.
24. Xia, Y. J.; Sun, K.; Ouyang, J. Y. Solution-Processed Metallic Conducting Polymer Filmsas Transparent Electrode of Optoelectronic Devices. *Adv. Mater.* **2012**, *24*, 2436–2440.
25. Wang, X. J.; Ishwara, T.; Gong, W.; Campoy-Quiles, M.; Nelson, J.; Bradley, D. D. C. High-Performance Metal-Free Solar Cells Using Stamp Transfer Printed Vapor Phase Polymerized Poly(3,4-Ethylenedioxythiophene) Top Anodes. *Adv. Funct. Mater.* **2012**, *22*, 1454–1460.
26. Lee, J. Y.; Connor, S. T.; Cui, Y.; Peumans, P. Solution-Processed Metal Nanowire Mesh Transparent Electrodes. *Nano Lett.* **2008**, *8*, 689–692.
27. Hu, L. B.; Kim, H. S.; Lee, J. Y.; Peumans, P.; Cui, Y. Scalable Coating and Properties of Transparent, Flexible, Silver Nanowire Electrodes. *ACS Nano* **2010**, *4*, 2955–2963.
28. Yu, Z. B.; Zhang, Q. W.; Li, L.; Chen, Q.; Niu, X. F.; Liu, J.; Pei, Q. B. Highly Flexible Silver Nanowire Electrodes for Shape-Memory Polymer Light-Emitting Diodes. *Adv. Mater.* **2011**, *23*, 664–668.
29. Zhu, R.; Chung, C. H.; Cha, K. C.; Yang, W. B.; Zheng, Y. B.; Zhou, H. P.; Song, T. B.; Chen, C. C.; Weiss, P. S.; Li, G.; Yang, Y. Fused Silver Nanowires with Metal Oxide Nanoparticles and Organic Polymers for Highly Transparent Conductors. *ACS Nano* **2011**, *5*, 9877–9882.
30. Dou, L. T.; You, J. B.; Yang, J.; Chen, C. C.; He, Y. J.; Murase, S.; Moriarty, T.; Emery, K.; Li, G.; Yang, Y. Tandem Polymer Solar Cells Featuring a Spectrally Matched Low-bandgap Polymer. *Nat. Photonics* **2012**, *6*, 180–185.
31. De, S.; Higgins, T. M.; Lyons, P. E.; Doherty, E. M.; Nirmalraj, P. N.; Blau, W. J.; Boland, J. J.; Coleman, J. N. Silver Nanowire Networks as Flexible, Transparent, Conducting Films: Extremely High DC to Optical Conductivity Ratios. *ACS Nano* **2009**, *3*, 1767–1774.
32. Xu, Z.; Chen, L. M.; Yang, G. W.; Huang, C. H.; Hou, J. H.; Wu, Y.; Li, G.; Hsu, C. S.; Yang, Y. Vertical Phase Separation in Poly(3-hexylthiophene): Fullerene Derivative Blends and its Advantage for Inverted Structure Solar Cells. *Adv. Funct. Mater.* **2009**, *19*, 1227–1234.
33. Kim, J.-Y.; Kim, S.-H.; Lee, H. H.; Lee, K.; Ma, W.; Gong, X.; Heeger, A. J. New Architecture for High-Efficiency Polymer Photovoltaic Cells Using Solution-Based Titanium Oxide as an Optical Spacer. *Adv. Mater.* **2006**, *18*, 572–576.
34. Park, M. H.; Li, J. H.; Kumar, A.; Li, G.; Yang, Y. Doping of the Metal Oxide Nanostructure and Its Influence in Organic Electronics. *Adv. Funct. Mater.* **2009**, *19*, 1241–1246.